IJHSR
ijhighschoolresearch.org
RESEARCH ARTICLE

Optimizing Blade Geometry for Vertical Axis Wind Turbines for Usage in Low-Speed Urban Environments

Edgar Salus

Berlin International School, Lentzealle 8-14, Berlin, 14195, Germany; edgar.heinrich.salus@gmail.com

ABSTRACT: In urban environments, such as Berlin, Germany, where wind is slow, turbulent, and multidirectional, conventional wind turbine designs often fail to operate effectively, especially during startup (Mertens). The challenge of effectively harnessing wind power in cities remains largely unsolved, despite multiple benefits: electrical infrastructure, undisturbed habitats, and proximity to where the electricity is most used (Stathopoulos *et al.*). Even though horizontal-axis wind turbines are more efficient than their vertical counterparts, especially at higher wind speeds, they are often deemed unsuitable for urban areas. However, vertical-axis wind turbines (VAWT) are more adaptive to changing wind directions because they don't require yaw and pitch adjustments (Al-Rawajfeh & Gomaa). This makes them more convenient for multidirectional gusts of wind, as is typically the case in urban areas. This study employs Computational Fluid Dynamics (CFD) to simulate the startup behavior of vertical-axis wind turbines at low air speeds. Since drag-based approaches have a faster startup response than lift-based vertical axis wind turbines (Darrieus blades), the geometry of the Savonius blade will be optimized to achieve the highest power output within a set time period.

KEYWORDS: Engineering, Aerodynamics, Vertical Axis Wind Turbine, Urban Environment, Efficiency, Computational Fluid Dynamics.

Introduction

In the face of accelerating urbanization and the ever-growing energy demand, the shift toward sustainable, decentralized energy sources has evolved into both a practical necessity and a strategic priority.[1] As cities expand and populations concentrate in metropolitan areas, the strain on centralized energy grids intensifies, increasing the urgency to reduce dependency on large-scale, fossil-fuel-based power plants.[2] Within this context, renewable energy technologies, particularly those capable of being deployed directly within cities, are positioned to serve a crucial function in enabling a resilient, low-carbon energy future.

Wind energy stands out as one of the most mature, reliable, and environmentally friendly forms of renewable energy available today. Traditionally, however, the majority of wind energy systems have been installed in rural landscapes or offshore locations, where the benefits of high and steady wind speeds, minimal obstructions, and reduced land-use conflicts can be fully leveraged.[3] While this deployment pattern has been instrumental in scaling global wind capacity, it has also left a big gap: the integration of wind turbines into densely populated urban environments remains limited.[4]

This underutilization is notable because urban wind energy offers considerable strategic advantages. By generating electricity close to the point of consumption, urban wind turbines can help reduce energy losses during transmission, lower peak demand on national grids, and increase resilience against large-scale outages or supply disruptions due to the possibility of multiple independent local grids. Furthermore, localized generation can support broader sustainability goals by complementing rooftop solar installations and contributing to a diversified, multi-source urban microgrid.[5]

Cities like Berlin, Germany, provide a particularly fertile ground for exploring small-scale wind energy harvesting. Their dense infrastructure, spanning rooftops, building facades, bridges, and transportation corridors, offers ample, underused surfaces and structural supports for turbine installation, eliminating the necessity for additional land use.[6] Moreover, the unique aerodynamics of urban landscapes can be turned from a challenge into an asset: air can be accelerated around corners, channeled between high-rise buildings, or induced by vehicular movement on busy streets.[7]

However, harnessing wind energy in urban areas is not without significant technical hurdles. Low average wind speeds, elevated turbulence intensity, and rapid fluctuations in wind direction make it difficult for wind turbines to operate efficiently.[4] These conditions demand systems capable of starting and generating power at low wind speeds (below 5 ms^{-1}), responding quickly to directional changes, and tolerating unsteady aerodynamic loads. Vertical-axis wind turbines (VAWTs), specifically Savonius-type configurations, offer inherent advantages in meeting these requirements. HAWTs require yaw adjustments to operate in areas with fast-changing wind directions, while VAWTs require no additional mechanisms to adapt. VAWTs also tend to operate more quietly, a crucial factor in maintaining community acceptance in noise-sensitive urban neighbourhoods.[8]

This study focuses on the city of Berlin, so the average annual wind speed of approximately 4.1 ms^{-1} was chosen to test the wind turbines.[9, 10] In an urban environment like Berlin, the wind direction changes on an hourly basis. This calls for

DOI: 10.36838/IJHSR811.48

two conditions: an omnidirectional design and a rapid startup, which are both possible with a VAWT. Therefore, the central aim is to improve start-up characteristics and operational responsiveness, and not the maximum possible angular velocity by optimizing the blade geometry of a VAWT. Short startup time is important, as changing wind directions mean short gusts of wind. Therefore, a higher power output after a certain amount of time was the most crucial factor for this study. A simple Savonius-type blade was taken and then iteratively designed to increase the peak moment, angular velocity, and hence power output within 150 seconds. 150 s was chosen as it provides an equal balance between short gusts of wind that typically last up to 30 seconds and slower, more constant wind that keeps blowing continuously. The changing wind directions were not considered within each simulation, as the VAWT is omnidirectional, but the VAWT performance was tested when the wind came from a different direction.

Principles of a Vertical-Axis Wind Turbine

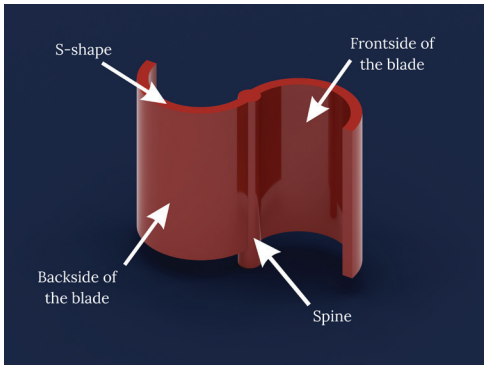

Figure 1: Synthetic Parts of a Savonius wind turbine, highlighting the core components involved in this study.

The Savonius wind turbine typically comprises two blades arranged around a central vertical shaft or spine. The blades form an S-shape from above, causing the front side of each blade to be concave and the back side to be convex, as shown in Figure 1.

When wind strikes the concave side of one of the blades, the curved surface traps more air, leading to a buildup of pressure, as illustrated in Figure 2. This pressure generates drag, which in turn exerts a force on the blade. Since the vertical spine of the turbine serves as the pivot point, this force produces a moment about the axis, initiating rotation. At the same time, the convex side of the opposing blade is also exposed to the wind. Although this side experiences airflow, its shape causes the air to pass over more smoothly, resulting in significantly lower pressure buildup. As a result, the force, and thus the opposing moment, or negative torque, is significantly weaker compared to the driving side. This imbalance between the stronger driving torque and the weaker resisting torque allows the turbine to rotate consistently in a single direction. Every time the blades sweep through the airflow, this process is repeated, sustaining the continuous motion of the Savonius wind turbine.

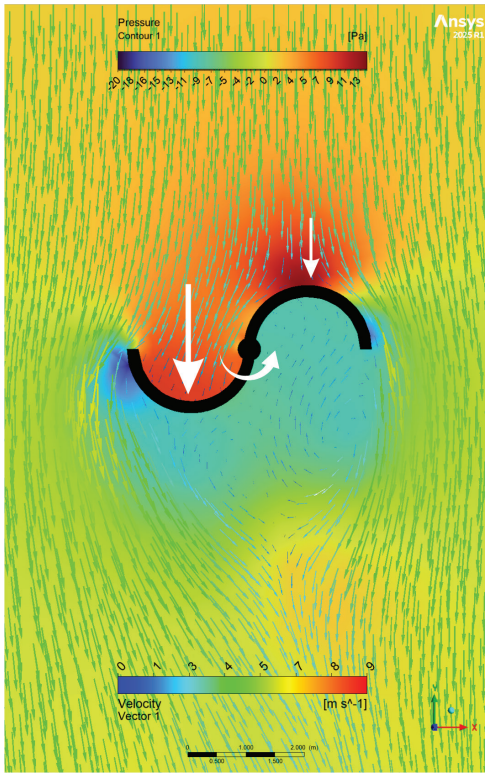

Figure 2: Forces acting on a Savonius VAWT. The imbalance between drag on the concave and convex sides produces a net torque that drives rotation.

There are various ways to increase the torque and angular velocity of the turbine: increasing the drag difference; increasing the distance between the forces and pivot point, to increase moment; reducing the moment of inertia of the wind turbine; and producing torque more consistently. Moment of inertia refers to the distribution of mass in relation to the rotational axis. A smaller moment of inertia means the object is less resistant to changes in its angular velocity. Mass further away from the rotational axis induces a higher resistance to changes in angular velocity, thus implying a slower start-up time. Thus, the efficiency of a Savonius wind turbine ultimately depends on maximizing the asymmetry between the driving and resisting forces while minimizing rotational resistance, thus allowing for a faster angular acceleration.

Methods

3.1. Experimental Setup and Tools:

For this study, the Ansys Fluent application was used for the CFD testing and Autodesk Fusion for the CAD modeling and other model-related calculations (moment of inertia, etc.).[11, 12]

These specific programs were chosen as they provide high compatibility and accuracy for engineering simulations, with Fusion enabling precise geometrical control and Fluent offering advanced turbulence and fluid interaction modeling.

In Autodesk Fusion, all models were created with two main parts: the blades and the central spine that would act as the turning axis. The same measurements for all models were applied:

- 4.2 m diameter of the entire wind turbine at its largest point

- 3 m high excluding spine (3.4 m with spine)
- central spine with 0.4 m diameter

These dimensions were selected to represent a small-scale turbine that would produce realistic aerodynamic behavior while keeping the computational load manageable. The proportions also ensured stability and minimized excessive tip effects during airflow analysis.

All models were assigned steel properties and then hollowed. The assumption that a 10mm thick wall would be sufficient to sustain all structures was not tested, as it was not included in the scope of this study. A moment of inertia for every design interaction for the turbine was calculated around the central rotational axis.

In Ansys Fluent, the watertight workflow was implemented to ensure accurate meshing and precise control over the simulation.

To create the meshes, a surrounding body was constructed. This body had the following dimensions: 5 times the diameter of the turbine downstream, double the diameter of the turbine upstream, and any of the other boundaries.

These boundary distances were chosen to eliminate external flow interference and ensure that wake development could occur naturally within the domain, avoiding reflections or artificial constraints on the airflow.

Growth rate, size of the mesh, and curvature normal angle were fixed to 1,1, 0.02, and 8 degrees, respectively, to ensure a high-quality mesh, even in the wake section.

3.1.1. Transient Simulations:

The viscous model used for all transient simulations was the realizable k-epsilon model with enhanced wall treatment. It is a two-equation turbulence model widely used in CFD simulations because it balances accuracy and computational efficiency.[13] Since this simulation involved rotating parts and keeping y+ in exactly the ideal range (y+ < 3) everywhere is difficult to achieve, the enhanced wall treatment was applied. This allowed the simulation to handle both fine meshes and coarser meshes without switching models for accurate near-wall effects, even with a coarser mesh.

The inlet speed was set at 4.1 ms^{-1}, which reflects the yearly average wind speed in Berlin over the entire year. As urban environments are categorized as turbulent environments, a turbulent intensity of 30%, and a viscosity ratio of 10 were chosen. To enable the wind turbines to spin freely, the 6DOF solver within Ansys Fluent was applied. This allowed the air particles to interact with the wind turbine and turn it around its specified axis. Given the correct moment of inertia from Autodesk Fusion, the startup behavior could now be simulated. The output parameters could be graphed against time and were set as follows:

- ω - angular velocity (rad s^{-1})
- T - torque (Nm)

Using this data, the power output could be calculated using the formula:

$P = T$

These parameters allow a fair evolution of each VAWT. All of these variables were tracked throughout the full 150 seconds of simulation time (unless otherwise specified). All transient simulations consisted of over 3000 timesteps, each 0.05 seconds long. Every simulation ran at least 20 iterations for every timestep, resulting in over 60,000 iterations for all transient simulations.

3.1.2. Steady Simulations:

For some modifications, only the drag of the concave and convex sides was tested. These simulations required far less computational time because they were steady rather than transient, which also made it possible to employ the more advanced transition SST viscous model, based on four governing equations. Each run was carried out for 200 iterations to ensure high reliability of results. The drag force of the convex and concave sides of the blade was tested individually, and then a difference was calculated. However, the difference in drag between the two sides was not sufficient to determine suitability, as the moment of inertia also significantly affects the turbine's angular velocity. For this reason, a ratio between the drag difference and the moment of inertia was calculated in every case, allowing the optimal balance between aerodynamic performance and rotational efficiency to be identified.

3.2. Variables:

To optimize the performance of the Savonius wind turbine, several design modifications were systematically tested to evaluate their effect on torque generation, rotational speed, and power.

Firstly, we investigated the number of blades, comparing the Savonius turbine designs with 2, 3, 4, and 5 blades. More blades should increase the smoothness of power output, but the increased number of blades will increase the moment of inertia significantly.

Secondly, the peak of the blades was offset outwards, as shown in Figure 3. This would shift the focus of the drag force experienced by the concave side further away from the pivot, thus increasing the torque. The peak was offset in 20 cm increments up to 60 cm.

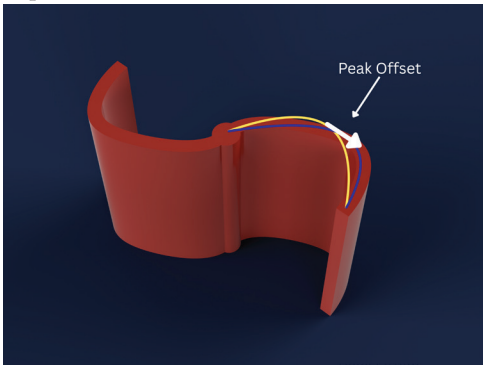

Figure 3: Offset outwards of the blade peak.

Thirdly, the geometry of the blade was manipulated in multiple ways to increase the difference in drag between the convex and concave sides of the blade. The first modification involved changing the peak radius of the blade illustrated in Figure 4. The radius was gradually increased in 10 cm increments, up to a maximum of 40 cm. Increasing the radius makes the

DOI: 10.36838/IJHSR811.48

concave side "deeper," allowing it to trap and redirect a larger volume of airflow, which results in higher pressure buildup and therefore higher drag. In contrast, the convex side becomes smoother with a larger radius, which encourages airflow to remain attached and slip past with relatively less resistance. This asymmetry enhances the difference in aerodynamic forces acting on the two sides of the blade, which is the driving principle of a drag-based turbine. By systematically increasing the peak radius (the depth of the blade), the balance between the drag difference of the concave and convex sides and the moment of inertia can be found.

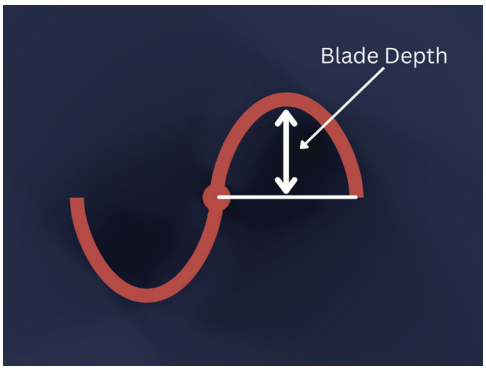

Figure 4: Variating the peak radius of the blade.

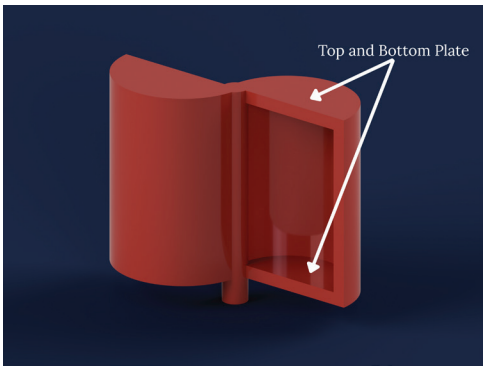

Figure 5: Adding top and bottom plates to the blades.

The fourth modification focused on attaching plates to the top and bottom edges of each blade, which is shown in Figure 5. These plates were designed to act as barriers that block air from escaping around the blade edges, forcing more of the airflow to interact with the concave surface. As a result, the concave side experienced even higher drag, while the convex side remained relatively unaffected. The design was refined through three iterations, each improving the positioning and geometry of the plates to maximize the drag difference while minimizing additional rotational momentum. By confining the airflow in this way, the plates served a similar function to endplates in aerodynamics, which are often used in wings and diffusers to reduce unwanted losses.

Finally, the best performing modifications based on the previous tests in this study were combined and tested for 150 seconds using the realizable k-epsilon model with enhanced wall treatment.

Results

4.1. The controlled case:

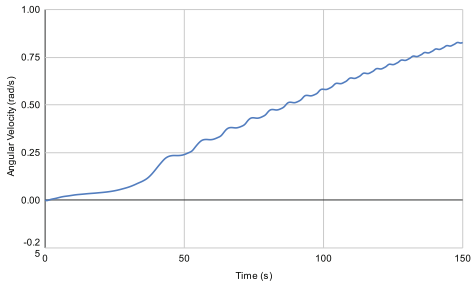

Figure 6: Angular velocity of the baseline Savonius turbine over time. The turbine accelerates gradually with strong oscillations within 150 s.

Firstly, the standard Savonius turbine was tested without any changes. Figure 6 shows the angular velocity over 150 seconds. The turbine ended up achieving an angular speed of 0.814 rad s^{-1}.

However, the angular velocity did not always increase. Instead, it changed in waves, with little peaks forming. This is due to the structure of this type of VAWT, due to the torque always changing and never staying constant, as shown in Figure 7. As time continues, these peaks become less prominent and more frequent because the turbine starts spinning faster. The faster spinning blades lower the peaks and troughs on the torque plot due to the relative speed between the blades and the surrounding air changing. The concave side creating most of the turning moment, starts moving with the wind, which decreases the relative speed of the air hitting the blade. This decreases the drag force on the blade, meaning less torque. On the other side, the convex side moves against the air flow. Hence, the relative speed between the blade and the air increases, increasing the drag force on the blade, meaning more torque working against the rotation. Therefore, the acceleration of the turbine slows until the forces acting on the concave and convex sides are in equilibrium.

Therefore, the power output of the VAWT fluctuates a lot, as shown in Figure 8. However, generator types like Double Fed Induction mean this is not an issue, due to their ability to easily being able to adjust to changing energy outputs.

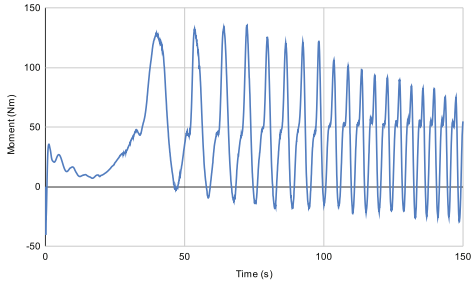

Figure 7: Torque of the Savonius turbine over time. The oscillatory torque profile explains the fluctuations observed in angular velocity and highlights the unsteady nature of drag-based VAWT operation.

4.2. Number of Blades:

The standard Savonius wind turbine design was tested with configurations of three, four, and five blades in order to evaluate how blade number influences startup behavior, angular velocity,

and energy output, and compared with the control. Across all cases, none of the turbines reached a steady-state speed within the 150 seconds of simulated runtime. Instead, each configuration was still in its startup phase, gradually accelerating under the influence of the wind. Nevertheless, the results still provided valuable insights into the comparative performance of different blade numbers, as each setup achieved significant angular velocities and torque outputs despite not reaching equilibrium.

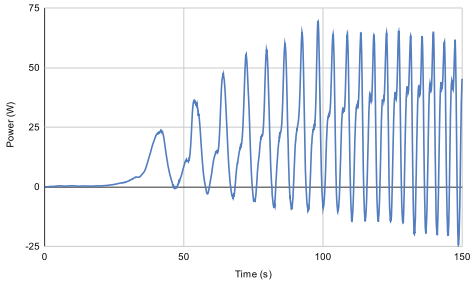

Figure 8: Power output of the Savonius turbine over time with strong fluctuations due to the unsteady torque and gradual increase in angular momentum.

The quantitative results of the blade number investigation are summarised in Table 1. The turbine with five blades performed the worst, producing the lowest maximum angular speed (0.533 rad s^{-1}), torque (102.3 Nm), and final energy output (26.1 W). The primary reason for this is its relatively large moment of inertia: with five blades distributed around the rotor, the turbine had more mass positioned farther from its axis of rotation, which substantially increased resistance to angular acceleration. Furthermore, with so many blades occupying the flow path, interference effects became prominent. As one blade attempted to capture airflow, adjacent blades obstructed or redirected part of that flow, leading to aerodynamic inefficiencies. Despite these drawbacks, the five-blade turbine displayed one noteworthy advantage: it was the first configuration to achieve noticeable angular speed, and its torque curve was the most stable and consistent. The overlapping operation of multiple blades smoothed out fluctuations and outputted power more consistently than the two-blade setup, which can be seen in Figure 8. This suggests that while the five-blade design is less efficient at maximizing power, it could be advantageous in applications where torque consistency is prioritized over peak performance.

In stark contrast, the two-bladed Savonius turbine delivered the best performance. It achieved the highest angular speed, the greatest peak torque, and the largest energy output. With only two blades, its moment of inertia was significantly lower than in the multi-blade cases, allowing it to accelerate more rapidly under the same wind conditions. Additionally, the reduced number of blades minimized aerodynamic interference, ensuring that each blade was exposed to a greater share of unobstructed airflow. However, one important factor influencing this result was the turbine's initial orientation. In the simulation, the blades were positioned perpendicular to the incoming wind, maximizing the drag difference between the convex and concave surfaces from the very start. Theoretically, if the turbine had instead started with its blades parallel to the wind direction, its initial torque would have been much lower. With less surface area directly exposed to the wind, the turbine would likely have taken longer to accelerate to meaningful angular speeds.

For turbines with three, four, or five blades, this orientation issue is irrelevant. Their symmetrical arrangements ensure that, regardless of the starting position, at least one blade will always face the airflow in a drag-producing orientation. To test the effect of orientation more rigorously, one additional simulation was performed on the two-bladed turbine. This time, the rotor was rotated 90 degrees so that the blades were parallel to the incoming wind, minimizing the exposed drag area at startup. Based on initial reasoning, this configuration was expected to perform worse, since it presented less effective surface area to the flow and should therefore have generated less torque in the early phase.

Table 1: Results of the blade number investigation. The two-bladed configuration achieves the highest angular velocity and power output due to its lower moment of inertia.

Number of Blades					
Number of Blades	Moment of Inertia (kg m^2)	Angular speed (rad s^{-1})	Peak moment (Nm)	Final moment (Nm)	Final power (W)
2.0	6,699	0.814	131.8	72.3	58.9
3.0	10,040	0.661	93.6	51.9	34.3
4.0	13,380	0.560	95.4	57.6	32.2
5.0	16,730	0.533	102.3	49.0	26.1
Starting position turned by 90 degrees					
2.0	6,699	0.925	128.5	74.5	68.9

Surprisingly, the results revealed the opposite: the two-bladed turbine actually performed better in this setup. Its angular velocity increased more rapidly, reaching 0.925 rad s^{-1}, and it achieved its first peak in rotational speed more than 70% earlier than in the perpendicular orientation. A likely explanation lies in the phenomenon of flow attachment. When the front-facing blade was aligned with the airflow, the air did not simply slip past it; instead, a portion of the flow adhered to the blade's curved surface, following its contour due to the Coanda effect. The attached flow redirected a significant portion of air into the concave surface of the trailing blade, as shown in Figure 9. Effectively, the leading blade acted as a guide vane, channeling airflow into the optimal region of the downstream blade and generating torque. This aerodynamic interaction gave the turbine a substantial head start, allowing it to spin up more quickly than in the perpendicular case.

DOI: 10.36838/IJHSR811.48

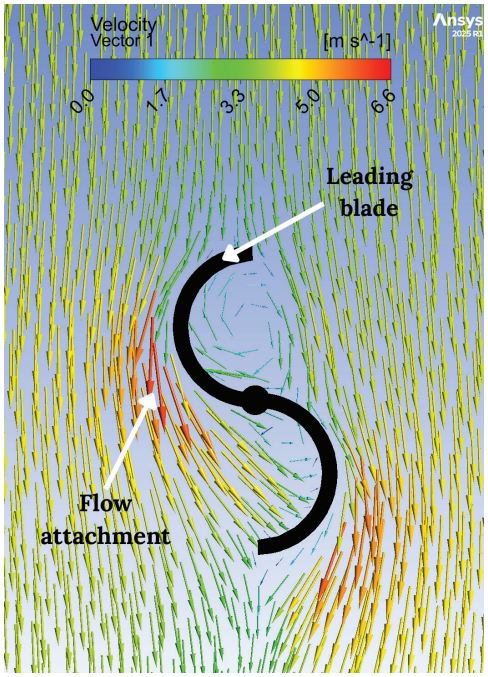

Figure SEQ Figure * ARABIC 9: Flow attachment on leading blade of VAWT, enhancing startup torque.

These findings suggest that parallel alignment can, in fact, yield superior acceleration due to flow redirection effects. Therefore, the orientation has little effect on the performance of the two-bladed VAWT, making it overall superior to its multi-bladed counterparts.

4.3. Peak Offset:

To investigate ways of increasing the torque generated by the turbine, the geometry of the blade was modified by offsetting the peak of its curve outward from the central axis. In a standard Savonius turbine, the blades are typically formed from semicylindrical shapes, where the peak of the curve lies directly on the diameter of the circle. By pushing this peak outward, the concave side of the blade becomes deeper and broader, thereby intercepting more of the incoming wind. In theory, this should allow the concave surface to capture a greater volume of airflow, producing higher drag and thus generating more torque. At the same time, the convex side of the blade becomes less curved and more elongated, changing how the wind interacts with that surface. This adjustment was tested at offsets of 20 cm, 40 cm, and 60 cm from the center, and the performance of these variants was compared to that of the standard, unmodified Savonius turbine.

The turbine with a 20 cm offset demonstrated the most promising results. In fact, it even outperformed the standard Savonius turbine in several important categories by a margin of approximately 8%. Its standout feature was its rapid startup behavior. Within the first 75 seconds of simulation, it reached an angular velocity of 0.58 rad s^{-1}, which is 34% higher than that achieved by the standard design over the same period. This faster acceleration translated directly into higher power output at early times, since power depends on both torque and angular velocity. The improved startup can be attributed to the enhanced aerodynamic asymmetry created by the moderate offset: the concave surface was able to generate stronger positive drag forces while the convex side, though slightly flatter, did not yet create excessive negative drag. As a result, the net torque driving rotation was maximized in the early stages. However, after 75 seconds, the 20 cm offset turbine experienced a relatively rapid decline in torque generation. Over longer simulation times (150 seconds), its average power output fell slightly below that of the standard turbine. This suggests that while the modified geometry provided a powerful initial boost, it also introduced aerodynamic inefficiencies at higher rotational speeds, such as greater turbulent losses and less favorable flow attachment on the convex surface.

In contrast, the turbines with larger offsets of 40 cm and 60 cm performed considerably worse. At first glance, the 40 cm offset seemed promising because it recorded the highest peak torque of all tested designs. However, this peak was achieved only after a long delay, and the turbine suffered from very poor startup characteristics. The higher moment of inertia associated with the outward displacement of the blade peaks meant that more energy was required to initiate rotation. Since rotational acceleration is inversely proportional to the moment of inertia (according to Newton's second law for rotation), the heavier, more extended blades were much slower to respond to the available torque. As a result, the turbine was unable to accelerate efficiently, undermining the advantage of its higher torque capability.

The 60 cm offset turbine performed even worse, with its angular velocity still close to zero after 75 seconds of runtime. This extreme underperformance cannot be explained by moment of inertia alone. The large offset altered the convex side of the blade geometry so dramatically that it effectively became a long, flat surface facing into the wind. Rather than allowing air to smoothly slip past, this flat surface caused significant flow stagnation and pressure buildup. In aerodynamic terms, the convex side was no longer "streamlined," and the flow separated early, creating a broad wake of turbulent, high-drag air behind it. The increased pressure drag on the convex side generated a large amount of negative torque, which directly counteracted the positive torque produced by the concave surface. This destructive interference between the two sides of the blade meant that much of the energy supplied by the wind was wasted, and the turbine struggled to overcome static resistance to rotation. Figure 10 illustrates this effect, showing the large pressure distribution on the convex face.

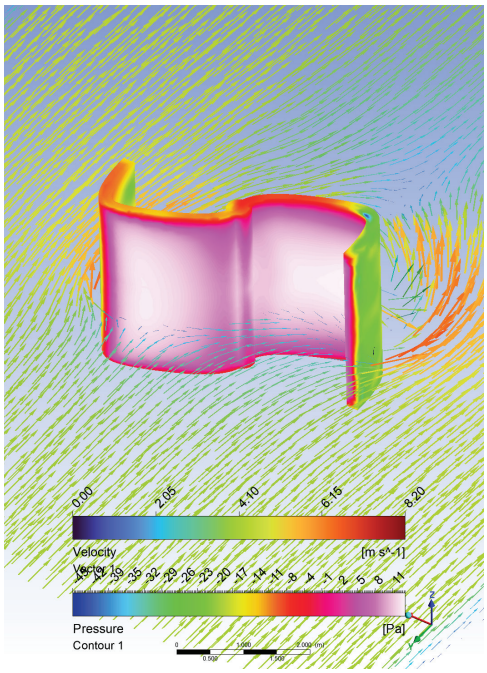

Figure 10: Pressure distribution on the turbine with a 60 cm peak offset. High pressure on the convex surface generates negative torque, significantly reducing startup performance.

A small outward offset, as in the 20 cm case, enhances moment asymmetry without excessively increasing convex-side resistance, thereby maximizing startup torque. But as the offset increases, the convex surface loses its curved, streamlined character and begins to behave like a flat plate, dramatically raising drag and producing counterproductive torques. At the same time, the greater offsets increase the turbine's moment of inertia, meaning even the torque that is available cannot translate into angular acceleration efficiently. The combination of these aerodynamic and mechanical effects explains why the 40 cm and 60 cm offsets performed so poorly in practice.

Table 2: Results of blade peak offset investigation. A 20 cm offset provides the best balance between increased torque and low moment of inertia.

Blade Offset to one side					
Amount of offset (cm)	Moment of Inertia (kg m²)	angular speed (rad s⁻¹)	Peak Moment (Nm)	Final Moment (Nm)	Final Power (W)
0.0	6,699	0.814	131.8	72.3	58.9
20.0	6,916	0.903	140.2	65.3	59.0
40.0	7,219	0.468	142.3	64.4	30.1
60.0	7,557	0.257	73.6	68.6	17.6

Overall, the offset modification demonstrated that careful geometric tuning can improve turbine performance, but only within narrow limits. The 20 cm offset represented a "sweet spot" where the increased drag asymmetry outweighed the penalties of higher inertia and convex-side drag. Larger offsets pushed the design past this optimum, creating negative aerodynamic interactions that prevented efficient startup.

4.4. Blade Depth:

The third set of modifications focused on altering the depth of the blade. The guiding idea behind these changes was to increase the difference in drag between the concave and convex sides of the blade, since this drag asymmetry is the driving force behind torque production in a Savonius turbine.

Interestingly, the standard Savonius blade performed surprisingly well. Despite having the lowest absolute drag difference of all tested geometries, it achieved the second-highest drag-to-inertia ratio. The explanation lies in its relatively low moment of inertia. Because the standard blade has a shallower depth, less of its mass is distributed far from the axis of rotation. This reduces rotational resistance, meaning that even a modest drag difference can translate into effective angular acceleration. In other words, although it does not maximize aerodynamic performance, the standard blade geometry benefits from being mechanically lightweight.

When the blade depth was increased to 1.1 meters, the performance improved significantly. This blade achieved the highest ratio score overall, outperforming the standard design. The reason was twofold: first, the convex side of the blade produced about 3.2 N less drag compared to the standard geometry. This reduction occurred because the deeper curvature of the blade promoted smoother flow separation, allowing air to slip around the convex side with less resistance. Second, the concave side experienced a slight increase in drag, which may seem counterintuitive at first. However, this is consistent with aerodynamic theory: the deeper blade provides a larger surface area for the wind to interact with, and more surface exposure typically increases form drag. Together, these changes widened the drag asymmetry, providing more useful torque without a disproportionate increase in inertia.

As blade depth continued to increase beyond 1.1 meters, the trend of larger drag differences persisted. However, the larger moment of inertia began to dominate. Since inertia grows approximately with the square of the distance of mass from the axis, deeper blades quickly became much harder to accelerate. This diminishing return meant that the deepest blades, despite having the largest aerodynamic drag differences, actually scored the lowest drag-to-inertia ratios. In practice, this highlights a key engineering trade-off: maximizing drag difference alone does not guarantee efficiency if the turbine becomes too mechanically sluggish to respond effectively to the wind.

Table 3: Results of the blade depth investigation. A blade depth of 1.1 m yields the highest drag-to-inertia ratio, indicating optimal startup efficiency.

Blade depth					
Peak Radius (m)	Moment of Inertia of full VAWT (kg m²)	Drag Frontside (N)	Drag Backside (N)	Drag Difference (N)	Ratio
1.0	6,699	108.3	45.42	62.9	0.00939
1.1	7,047	108.7	42.17	66.5	0.00944
1.2	7,741	109.2	40.32	68.8	0.00889
1.3	8,509	109.3	38.91	70.4	0.00827
1.4	9,353	111.9	37.71	74.1	0.00793

4.5. End plates:

The fourth set of modifications tested the effect of adding end plates to the blades. End plates are often used in aerodynamic design because they limit the escape of airflow around the blade tips, thereby reducing tip vortices and improving the

DOI: 10.36838/IJHSR811.48

effective drag on the concave side. This design was refined over three iterative steps; each balancing drag performance with moment of inertia.

The first iteration of end plates was not particularly successful. Although the plates reduced the drag on the convex side by suppressing the low-pressure wake behind it, they also inadvertently decreased the drag on the concave side. With less air circulation being trapped inside the concave surface, the pressure differential was smaller than expected. Since both drag contributions dropped, the net drag difference increased only slightly. Unfortunately, this minor aerodynamic gain was offset by the substantial increase in moment of inertia introduced by the heavy plates. As a result, this design scored lower than even the standard turbine in terms of ratio performance.

In the second iteration, many of the sharp edges of the plates were filleted, as shown in Figure 11. This adjustment made a profound difference. By smoothing the flow path, the fillets reduced turbulence around the blade and improved pressure build-up on the concave side. At the same time, the rounded geometry allowed air to pass more cleanly around the convex side, further lowering its resistance. This combination created a stronger drag asymmetry, while the reduced mass of the plates slightly lowered the turbine's moment of inertia. The result was a dramatic improvement, with the iteration achieving a ratio score nearly 37% higher than the previous design.

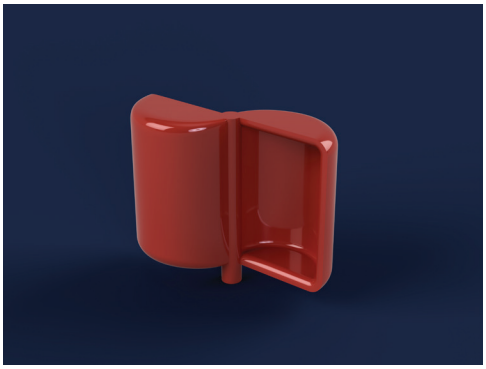

Figure 11: Second iteration of the end plate design. Filleted edges improve airflow attachment and increase drag asymmetry compared to the first iteration.

The third iteration refined the design even further by reducing the size of the plates (Figure 12). This modification sought to preserve the aerodynamic benefits of the earlier design while cutting down on mass to minimize inertia. The smaller plates maintained favorable airflow patterns, continuing to suppress turbulence and guide more wind into the concave side. At the same time, their reduced size meant that the moment of inertia was actually lower than that of the standard turbine. This combination of aerodynamic efficiency and mechanical responsiveness produced the highest ratio score of all tested geometries, outperforming the standard turbine by nearly 30% and the first plate design by an impressive 43%.

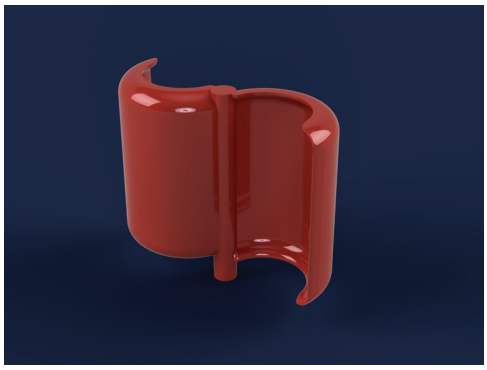

Figure 12: Third iteration of the end plate design. Reduced plate size preserves aerodynamic benefits while lowering moment of inertia, leading to improved overall performance.

Table 4: Results of the end plate study. The third iteration achieves the highest drag-to-inertia ratio by combining aerodynamic improvement with reduced inertia.

Endplates					
Design Iteration	Moment of Inertia of full VAWT (kg m²)	Drag Frontside (N)	Drag Backside (N)	Drag Difference (N)	Ratio
1	7,651	105.7	40.85	64.9	0.00848
2	7,145	109.6	26.57	83.0	0.01161
3	6,461	103.4	25.07	78.4	0.01213

4.6. Final Designs:

Drawing on the insights gained from the various geometric modifications, a final design was established by combining the most effective features: the third plate iteration, the 1.1 m blade depth, and a 20 cm peak offset, as depicted in Figure 13. In theory, this configuration should maximize drag asymmetry while limiting the mechanical downsides of an increased mass distribution, thereby producing a Savonius turbine with both strong startup torque and limited resistance to angular acceleration.

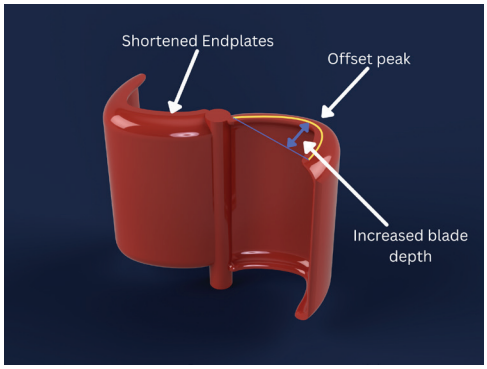

Figure 13: Final optimized Savonius turbine design. The geometry combines the most effective modifications to balance drag asymmetry and rotational inertia.

When tested, the final design did indeed outperform the standard Savonius turbine, although to a lesser degree than predicted. The optimized geometry produced a 16% higher peak torque, a 0.7% increase in peak angular velocity, and a 4% higher final power output after 150 seconds of simulation. These gains confirm that geometric refinement can yield improvements in turbine efficiency. However, the improvements

fell short of expectations, which can be attributed primarily to the higher moment of inertia introduced by the combined modifications and the standard Savonius turbine already being quite optimized as is.

From a physics perspective, the startup behavior of drag-based turbines is governed by the balance between aerodynamic drag differential (the torque-producing force) and rotational inertia (the resistance to angular acceleration). While the final design achieved the highest torque of all tested geometries, it also carried a 5% higher moment of inertia than the standard configuration. This higher moment of inertia acted as a bottleneck, slowing down acceleration and preventing the turbine from fully capitalizing on its aerodynamic improvements during the simulation time frame. The importance of this trade-off is highlighted by the performance of the 20 cm offset turbine tested earlier: despite not having the highest torque, its relatively low inertia enabled it to achieve a much higher angular velocity than other designs within the first 75 seconds, demonstrating that startup responsiveness can often outweigh peak torque in determining overall efficiency.

Conclusion

This study set out to investigate the aerodynamic optimization of Savonius-type vertical axis wind turbines (VAWTs) for potential use in low-speed, turbulent, and multidirectional urban environments, such as Berlin. Using computational fluid dynamics (CFD) simulations, several geometric modifications were tested, including variation in blade number, peak offsets, blade depth, and the addition of end plates. The results confirm that small geometric changes can have disproportionately large effects on turbine performance, particularly in the startup phase, where drag asymmetry and inertia compete to determine acceleration.

Several key findings emerged. First, reducing the number of blades to two improved startup performance by minimizing aerodynamic interference and rotational inertia, though at the cost of torque smoothness. Second, moderate peak offsets (20 cm) provided a "sweet spot" where torque was enhanced without generating excessive drag on the convex side, while larger offsets (40–60 cm) proved detrimental due to flow separation and negative torque. Third, increasing blade depth to 1.1 m improved drag asymmetry, primarily by reducing convex-side resistance, though further increases became counterproductive as inertia scaled faster than aerodynamic benefit. Finally, the addition of end plates, particularly in the third design iteration with reduced plate size and filleted edges, proved highly effective in improving drag difference while simultaneously lowering turbulence and moment of inertia.

The final optimized design, which combined these modifications, demonstrated measurable improvements in torque, angular velocity, and power output compared to the baseline turbine. However, the gains were more modest than anticipated. This result highlights the fundamental design trade-off in Savonius turbines: enhancing drag asymmetry inevitably increases mass distribution, which raises moment of inertia and limits startup acceleration. Successful optimization, therefore, requires carefully balancing aerodynamic improvements with mechanical responsiveness.

Looking forward, several directions for further research can be identified:

1. Reducing Moment of Inertia:

Future designs should aim to lower inertia without compromising structural stability, for example, by using lighter composite materials. This would improve startup performance, especially in low wind conditions.

2. Exploiting Flow Attachment Effects:

Some simulations revealed that flow attachment and redirection could dramatically enhance startup torque. Developing blade geometries that deliberately channel airflow between blades may unlock new performance gains at low wind speeds.

3. Finer Incremental Testing:

Smaller design changes (e.g., 5 cm offsets instead of 10 cm) should be tested to map performance trends with greater precision. This would help identify subtle optima that may be missed with larger increments.

4. Wake and Array Studies:

Since urban deployment often requires multiple turbines in proximity, future work should investigate the wake interactions of optimized designs. Understanding how turbines perform in series or clusters will be crucial for real-world feasibility.

5. Scaling and Dimensioning:

Finally, an important avenue is to determine the optimal size of Savonius turbines for urban areas. Larger rotors capture more wind energy but increase inertia and structural demands, while smaller turbines may respond better to turbulent urban flows.

In conclusion, while the optimized turbine presented in this study shows clear improvements over the standard Savonius design, it also underscores the complexity of balancing aerodynamic and mechanical factors in VAWT optimization. Future research that integrates aerodynamics, materials science, and urban flow modeling will be essential in developing efficient, robust, and scalable turbine solutions for the built environment.

Acknowledgments

I would like to express my special gratitude towards Dr. Devin Carroll and Kieran Tait for their valuable feedback, motivation, and trust in me to finish my paper in time. I would also like to thank the IRIS education team.

References

1. *World Energy Outlook 2021 – Analysis. IEA. https://www.iea.org/reports/world-energy-outlook-2021* (accessed 2025-08-22).
2. Chu, S.; Majumdar, A. Opportunities and Challenges for a Sustainable Energy Future. Nature **2012**, 488 (7411), 294–303. https://doi.org/10.1038/nature11475.
3. Tumse, S.; Bilgili, M.; Yildirim, A.; Sahin, B. Comparative Analysis of Global Onshore and Offshore Wind Energy Characteristics and Potentials. Sustainability **2024**, 16 (15), 6614. https://doi.org/10.3390/su16156614.
4. Mertens, S. Wind Energy in Urban Areas: Concentrator Effects for Wind Turbines Close to Buildings. Refocus **2002**, 3 (2), 22–24. https://doi.org/10.1016/S1471-0846(02)80023-3.

DOI: 10.36838/IJHSR811.48

5. Tsionas, I.; Llaguno-Munitxa, M.; Stephan, A. Environmental Effects of Urban Wind Energy Harvesting: A Review. Buildings & Cities **2025**, 6 (1). https://doi.org/10.5334/bc.491.
6. Wilke, A.; Shen, Z.; Ritter, M. How Much Can Small-Scale Wind Energy Production Contribute to Energy Supply in Cities? A Case Study of Berlin. Energies **2021**, 14 (17), 1–20.
7. Stathopoulos, T.; Alrawashdeh, H.; Al-Quraan, A.; Blocken, B.; Dilimulati, A.; Paraschivoiu, M.; Pilay, P. Urban Wind Energy: Some Views on Potential and Challenges. Journal of Wind Engineering and Industrial Aerodynamics **2018**, 179, 146–157. https://doi.org/10.1016/j.jweia.2018.05.018.
8. Al-Rawajfeh, M. A.; Gomaa, M. R. Comparison between Horizontal and Vertical Axis Wind Turbine. IJAPE **2023**, 12 (1), 13. https://doi.org/10.11591/ijape.v12.i1.pp13-23.
9. Berlin Climate, Weather By Month, Average Temperature (Berlin, Germany) - Weather Spark. https://weatherspark.com/y/75981/Average-Weather-in-Berlin-Germany-Year-Round (accessed 2025-08-13).
10. Accurate Berlin Wind Forecast | See Average Wind Speed. World Weather & Climate Information. https://weather-and-climate.com/average-monthly-Wind-speed,Berlin,Germany (accessed 2025-08-13).
11. Ansys Fluent – Computational Fluid Dynamics Software. Ansys Inc. https://www.ansys.com/products/fluids/ansys-fluent (accessed 2025-08-11).
12. Autodesk Fusion – Integrated CAD, CAM, and CAE Software. Autodesk Inc. https://www.autodesk.com/products/fusion-360/overview (accessed 2025-08-10).
13. Rezaeiha, A.; Montazeri, H.; Blocken, B. Towards Accurate CFD Simulations of Vertical Axis Wind Turbines at Different Tip Speed Ratios and Solidities. Renewable and Sustainable Energy Reviews **2019**, 111, 1–17. https://doi.org/10.1016/j.rser.2019.05.030.

Author

Edgar Salus is a senior at Berlin International School, Germany. He is deeply passionate about physics, engineering, and entrepreneurship. His recent projects include founding the Quantum, leading JEC Berlin, founding an online business for field hockey equipment, and managing the F1 in Schools team. Edgar seeks to major in mechanical engineering.